Study on the Changes in the Intermolecular Interactions of a Rod−Coil Liquid Crystalline Oligomer Using Raman Spectroscopy

Soo-Chang Yu,*,† Yonggak Choi,† Keunok Han Yu,† Jongwan Yu,† Hosoeb Choi,† Dong Hee Kim,† and Myongsoo Lee‡

Department of Chemistry, Kunsan National University, Kunsan, Chonbuk 573-701, Korea; and Department of Chemistry, Yonsei University, Sinchon 134, Seoul 120-749, Korea

Received November 16, 1999; Revised Manuscript Received May 22, 2000

ABSTRACT: The intermolecular interactions between neighboring liquid-crystalline molecules, the esterification products of ethyl 4-[4′-oxy-4-biphenylcarbonyloxy]-4′-biphenylcarboxylate with poly(ethylene oxide)s (PEO) (DP = 12), were investigated using micro-Raman spectroscopy. To this end, the experiment was performed under the two different conditions, i.e., salt and temperature variations. We found that the modification of mesogenic Raman bands is mainly attributed to the changes in intermolecular interactions. The hydrogen bonding between the C═O functional group near the ethyl terminal and one of the hydrogen atoms in the PEO unit nearest the mesogenic moiety is responsible for the intermolecular interactions which affect the molecular packing. Van der Waals interaction is also taken into consideration in interpreting the experimental results. We suggest a mechanism for the conformational change during the solid-to-liquid crystal transition based on a systematic investigation of the related molecules.

1. Introduction

Liquid crystalline polymers (LCPs) have been intensively studied for their scientific and technological interests. Among LCPs, rod−coil type molecules have recently drawn attention, particularly in relation to their properties to form various kinds of supramolecules depending on chain lengths.[1−8] Rod−coil molecules, consisting of a rigid rod block and a flexible coil block, can provide a novel class of self-assembling materials; the molecule shares certain general characteristics of both diblock molecules and thermotropic calamitic molecules.

LCPs based on a biphenyl ester moiety can have various microscopic structures; most poly(ethylene oxide)s (PEO)-based LCPs result in a layered smectic mesophase,[6] whereas poly(propylene oxide)s (PPO)-based LCPs result in a layered smectic C, smectic A, biconticuous cubic, and hexagonal columnar mesophases, depending on chain lengths.[7] Generally, a microphase formation is closely related to the molecular arrangement, the molecular conformation, and the intermolecular interactions. Therefore, the molecular-based information on the intermolecular interactions between LCPs is very important to get an insight into the mechanism for the formation of supramolecules.[9]

LCPs containing ester functional group in a mesogenic unit have long been the subjects for the studies of intermolecular interactions. There have been lots of theoretical and experimental works performed to identify the planarity between the benzene rings and adjacent carbonyl groups, and also the location of bond rotation above the phase transition (solid-to-liquid crystal).[10−16] Vibrational spectroscopic techniques such as infrared and Raman are considered among the most efficient tools to obtain rich vibrational information at the molecular level. For morphological study, the Raman spectroscopic technique is recognized to be superior to the infrared method because no modification to the sample is incurred during Raman measurement, which is critical to the preservation of the morphology.[17]

To study the modification of the intermolecular interactions between the mesogenic units in a rod−coil type LCPs, we preliminarily studied the effects of salt and temperature on the microstructural change of 12−4 (Figure 1) using micro-Raman spectroscopy, and found that unbound salt acts as a spacer, thus reducing the intermolecular interactions.[18] An in depth study is required to better understand the mechanism for the conformational change accompanied by the modification of intermolecular interactions.

In this paper, we recorded Raman spectra on the 12−4 analogues as depicted in Figure 1, and made a comparison with that of 12−4. A plausible mechanism for the conformational changes of a mesogenic unit is suggested based on these results.

2. Experimental Section

The chemical structures of 12−4 and its analogues are shown in Figure 1. The details of the synthesis and characterization of 12−4, and the preparation of the complexes of 12−4-salt were reported in the previous publication.[6,8] 12−4 analogues were synthesized based on the procedure of 12−4 with some minor modifications. A Perkin-Elmer DSC-7 differential scanning calorimeter(DSC) equipped with a 1020 thermal analysis controller was used to determine the thermal transitions.The heating rate was 10 °C min^{-1}.

The Raman spectra were obtained using a Renishaw Raman micro system 2000 with an excitation source of the 632.8 nm line of a HeNe laser. The laser power at the sample was ca. 5 mW and the spectra were recorded for 20−50 scans depending on the samples. The resolution of the spectra was within ±2 cm^{-1}. All the samples were put on glass slides, and the data were acquired by using an Olympus 20× objective lens. By using 632.8 nm excitation source, we took advantage to get the luminescence signal for the liquid crystalline samples, which cannot be obtained by FT-Raman experiment. A Linkam heating and freezing stage (THMSE 600) with a controller (TMS 92) was used for temperature control. All the spectra were calibrated to the silicon band at 521 cm^{-1} and manipulated with the software provided by Renishaw. Background

* To whom correspondence should be addressed.
† Kunsan National University.
‡ Yonsei University.

10.1021/ma991933m CCC: $19.00
Published on Web 08/01/2000

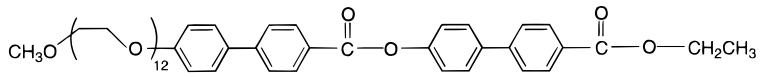

12-4

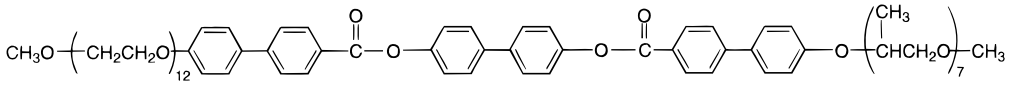

12-6-P7

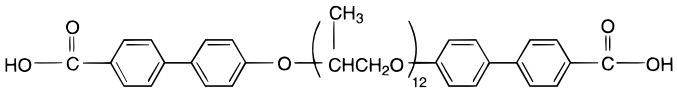

2-P12-2

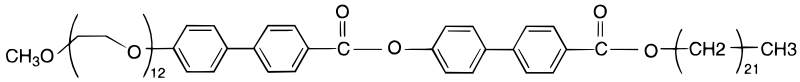

550-22

Figure 1. Molecular structures of 12−4 and its analogues.

corrections were made as needed. Band deconvolution was performed using a commercial program, *Grams 32*, to separate multiple components with a band shape being a mixture of Gaussian and Lorentzian functions.

3. Results and Discussion

To study the conformational change during the LC phase transition (solid-to-liquid crystal), temperature-dependent Raman spectra were obtained. Phase transition temperature was checked by plotting the intensity change of the aromatic Raman bands as a function of temperature. The bands belonging to the mesogenic units are known to be characteristic of the phase transitions; we selected the 1184 cm^{-1} band, the CH in-plane bending mode, as a representative of the aromatic modes. This band was normalized to the biggest band at 1599 cm^{-1}, which is assigned to the aromatic C═C stretching mode as represented in Figure 2. The temperature-dependent change of this band shows an abrupt drop near 137 °C. Likewise, the other mosogenic bands behaved similarly. It is also noteworthy that the luminescence intensity increases at the same temperature, and the crossing point between the two curves is found to be almost the same as the solid-to-smectic transition temperature (Sc = 135.2 °C) measured by a DSC experiment.[6,8] The luminescence background attributed to unknown origin overshadows the Raman signal for polymer materials when a light source in the visible region like 514.5 nm is employed.[19] The longer wavelength of 632.8 nm than 514.5 nm as an excitation source, however, allowed us to monitor the behavior of informative luminescence as well as Raman scattering. The abrupt increase in intensity of the luminescence seems to be due to the recovery from the self-quenching as the spacing is getting wider between the neighboring molecules with increasing temperature. Therefore, the Raman technique is quite compatible with DSC technique to determine the phase transition temperature.

It is known that the mesogenic conformational changes are mostly responsible for the differences between the adjacent crystalline polymorphs in liquid crystalline molecules.[20,21] Therefore, of particular interest are the mesogenic Raman bands reflecting mesogenic conformational changes with the environmental changes such as temperature and salt concentration.

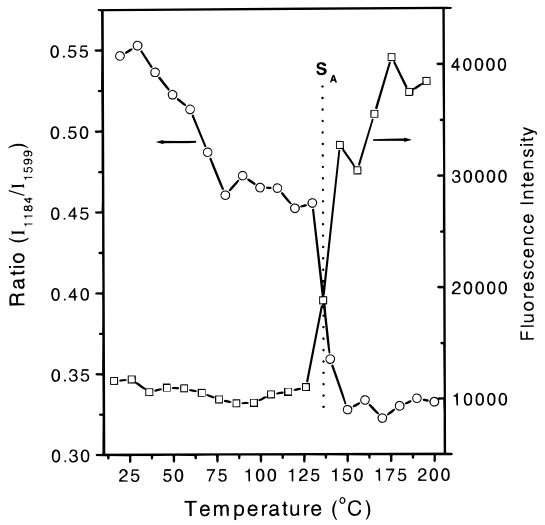

Figure 2. Intensity changes of the normalized aromatic Raman (left) and luminescence bands (right) as a function of temperature. The cross point at 137 °C is in good agreement with the phase transition temperature (135.2 °C) obtained from DSC measurement.

A systematic approach was used to see the effect of salt on the conformational changes. The binding of $LiCF_3SO_3$ to 12−4 was checked by observing the behavior of the SO_3 stretching bands. In the 12−4 matrix, the salt may exist as three different types depending on its concentration;[22,23] free ion of $CF_3SO_3^-$, ion pair of $Li^+CF_3SO_3^-$, and self-aggregate of ion pairs. Among the corresponding Raman bands, the bands at 1033, 1043, and 1052 cm^{-1} are assigned to free ion, ion pair, and self-aggregate forms, respectively. Therefore, only

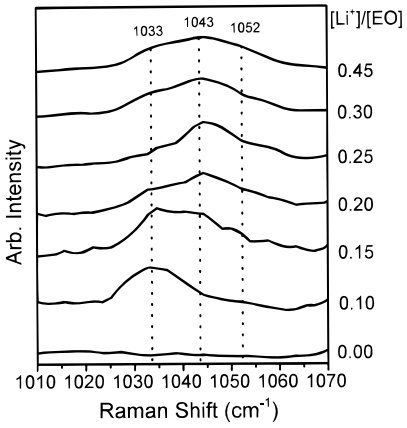

Figure 3. SO_3 stretching modes with different $[Li^+]/[EO]$. The detailed explanations are described in the text.

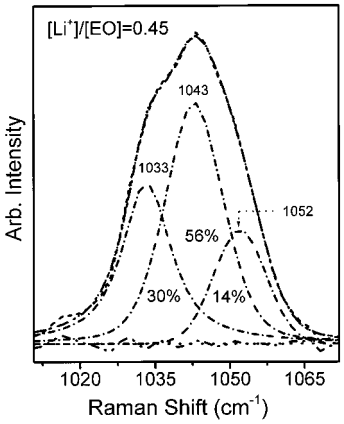

Figure 4. Curve-fitted spectrum of the SO_3 stretching band at $[Li^+]/[EO] = 0.45$. The fraction of each band is calculated from the integrated band area out of the total intensity.

the 1033 cm^{-1} band is expected to appear, provided that the salt binds to 12−4 completely at low salt concentrations, whereas the other two bands are expected at higher concentrations. This is manifested by the results shown in Figure 3, showing that the salt exists only in the completely dissociated form when $[Li^+]/[EO]$ is 0.1, where $[Li^+]$ and [EO] represents the concentration of the Li^+ ion and ethylene oxide unit, respectively, and the contribution from the other bands increases as the $[Li^+]/[EO]$ value increases between 0.15 and 0.45.

Spectral analysis of the SO_3 stretching Raman band at $[Li^+]/[EO] = 0.45$ shows that it decomposes into the three components; the 1033, 1043, and 1052 cm^{-1} bands attribute 30%, 56%, and 14%, respectively, to the total integrated area of Raman band as shown in Figure 4. Per unit EO moiety, the portion of the unbound salt is calculated to be 0.13 (30% of 0.45), which is in accordance with the results observed in Figure 3, where the concentration of completely dissociated salt is observed to be between 0.10 and 0.15. Thus, we conclude that the unbound salt acts as a spacer between neighboring 12−4 molecules, which leads to the modification of the intermolecular packing structure in the matrix.

Although it is widely accepted that the Li^+ ion binds to the oxygen atom in PEO chain, it is necessary to explore the possibility of forming the complex between the Li^+ ion and the C═O group.[24] In this regard, the temperature-dependent evolution of the C═O band in 12−4-salt complex ($[Li^+]/[EO] = 0.45$) was compared with that of salt-free 12−4 and was shown in Figure 5.

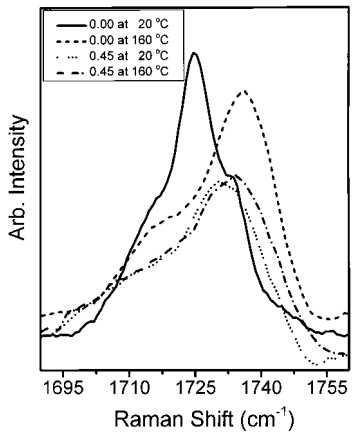

Figure 5. Temperature dependence of the C═O stretching band at $[Li^+]/[EO] = 0.45$ and 0.

The progression of the band that originated from the salt complex shows no dramatic changes in both intensity and frequency with increasing temperature as opposed to that of the salt-free band. We proposed that if the complex was formed between the Li^+ ion and the C═O group, the frequency and intensity recovery, then, should have occurred with increasing temperature since the population of the free C═O would be increased. Therefore, no dramatic change in either frequency or intensity of the C═O band allows us to conclude that there is no salt-bound C═O mode in this system. A decrease in intensity of the C═O band upon addition of salt is thought to be mainly attributed to the change in the optical activity induced rather by the excess salt than by the formation of complex.

The formation of the salt complex is well-known to occur through the oxygen atoms of the PEO chain.[25−28] As the metal cations bind to the oxygen atoms, the conformational change of the PEO unit brings about the different sequence of cis and trans conformers. As a result, either the frequency or intensity of the rocking and bending vibrations changes the $-CH_2$ in the PEO chain in the spectral range 800−900 cm^{-1}. In addition to this range, we observed other spectral modifications in the other spectral region, which has not been previously reported as far as we know. These observations are variations of the symmetric and asymmetric C−H stretchings of PEO at 2878 and 2934 cm^{-1}, respectively, as shown in Figure 6. The main difference in the spectral behavior under the two conditions, i.e., the salt and temperature variations, is the relative intensity change between the symmetric and asymmetric bands. The relative intensity is somewhat invariant with increasing temperature, and varies significantly with increasing salt concentration. This indicates that the Li^+ does indeed bind to the oxygen atoms, and induces a perturbation in the adjacent C−H stretching vibrations.

The degree of intermolecular packing between the neighboring molecules can be studied by observing the characteristic vibrational modes in the range 1130−1350 cm^{-1} (Figure 7). As previously reported,[18] the bands originating from the mesogenic units vary with the environmental changes such as temperature increase or salt addition. Emphasis should be placed on the bands at about 1274 cm^{-1} to reveal the mechanism for the conformational change during the phase transition because band splitting is clear with the environmental changes. This band, which is assigned to the

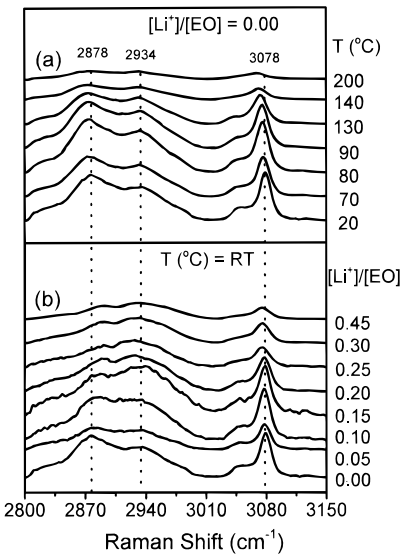

Figure 6. Profile of the C−H symmetric and asymmetric stretching bands of PEO unit at 2878 and 2934 cm^{-1}, respectively, and of the aromatic C−H stretching band at 3078 cm^{-1} with the variations of temperature (a) and salt (b).

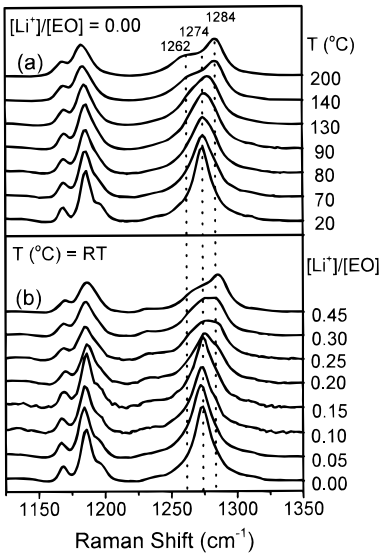

Figure 7. Profile of the combination mode of the aromatic C−C(═O)O and *C*(═O)O stretching vibrations in the range 1130−1350 cm^{-1} with the variations of temperature (a) and salt (b).

combination mode of the aromatic C−C(═O)O and *C*(═O)O stretching vibrations, is due to overlapping of the two bands originating from the two ester groups located on both sides of a biphenyl group when no perturbation is exerted. As the degeneracy is removed as a result of bond rotation about the C═O group near the ethyl terminal, the single band splits into two bands due to the appearance of the two distinguishable conformers with respect to the biphenyl group surrounded by two ester groups. This is achieved by reorientation of the molecules upon breaking the intermolecular interactions in the crystalline melt.

Several schemes may be suggested for the bond rotation as depicted in Figure 8. The first possibility could be the rotation about the phenyl−phenyl bond next to the ethyl ester group (rotation ①): a second possibility is the rotation about the aromatic carbon−carbonyl carbon bond (rotation ②): a third possibility

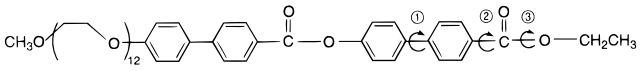

12-4

Figure 8. Schematic diagram for the possible bond rotations.

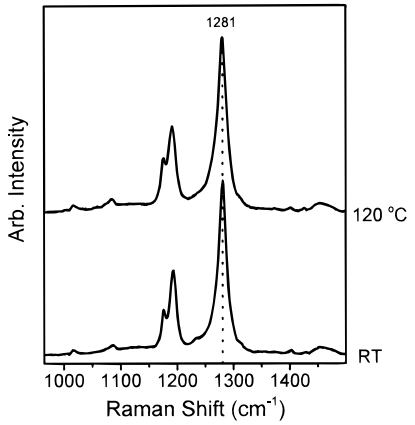

Figure 9. Spectra of 12−6-P7 at low and high temperatures. No spectral splitting is occurred above the phase transition temperature at 110 °C measured by DSC in a heating scan.

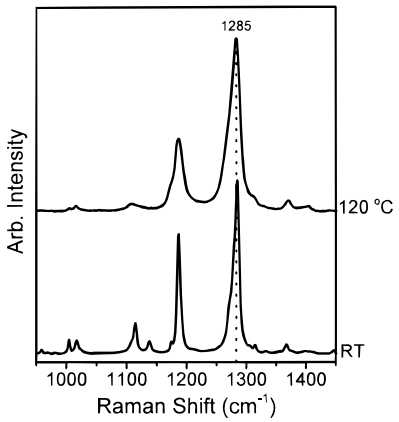

Figure 10. Spectra of 2-P12−2 at low and high temperatures. No spectral splitting occurred above the phase transition temperature at 67 °C measured by DSC in a heating scan.

is the rotation about the carbonyl carbon−ester oxygen bond (rotation ③). The first possibility initially appears to be plausible because the activation energy needed for the bond rotation since the bond connecting the phenyl rings has a single character in bond order; however, the steric strain must be very large for the benzene ring to rotate in a well-ordered condensed phase. Therefore, the first possibility is unacceptable. Further support for this conclusion was given by taking Raman spectrum of 12−4 analogue, 12−6-P7, as shown in Figure 1. 12−6-P7 is very similar to 12−4, with the exception of a heavier moiety instead of ethyl ester at the end. Considering the molecular structure of 12−6-P7, the conformers of *C*(═O)O are to be generated if rotation ① occurs resulting in the band splitting above the transition temperature. The spectrum in Figure 9, however, shows no change in intensity or frequency indicating that rotation ① can be neglected in our molecular system. For the second possibility, similar models in other research suggest similar arguments. Del Pino et al.[14] claimed that rotation ② is not plausible because the C═O group is positioned parallel to the phenyl plane with partial double bond character be-

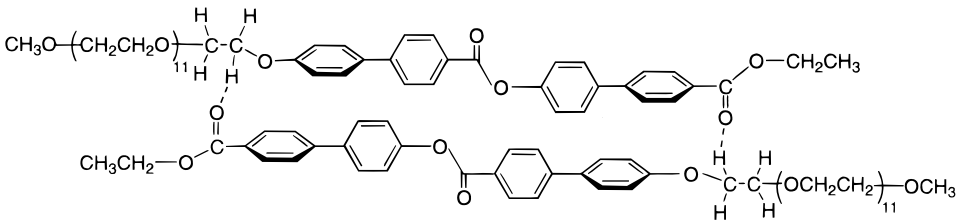

Figure 11. Schematic diagram for the hydrogen bonded dimer of 12−4 inferred from a simple molecular modeling.[33] To simplify the calculation, only one PEO unit is adopted out of 12 units. The dotted line indicates the plausible hydrogen bonding.

tween the aromatic C and *C*(═O)O due to the resonance with the adjacent aromatic ring. In contrast, Ozaki et al.[29] addressed the possibility of rotation ② from his time-resolved IR spectra. Our previous study also suggested that the second possibility agreed with the latter result.[30] In our spectrum, the band splitting was observed to evolve slowly with increasing temperature as the ethyl terminal(12−4) was replaced with a longer alkyl chain (550−22, to be mentioned in the following paragraph). This band splitting was ascribed to rotation ② because the degeneracy was removed as a result of the conformer generated around the *C*(═O)O groups. The third possibility can be ruled out because rotation ③ will not give rise to conformers of the neighboring C═O groups. For example, Jedlinski et al.[16] investigated the effect on the conformational change of ether and ester bonds linking an aromatic mesogenic unit and a flexible spacer in poly(ether ester) liquid crystals. They found that the conformational change occurs only in the case of ester bonds. A similar behavior was observed in 2-P12−2 of which C═O groups are apart so that the conformers may not be easily generated. In this case the band shape at high temperature hardly changes compared to that at low temperature except for a slight thermal broadening (Figure 10). To further clarify, vibrational frequency calculations are needed for both the cis and trans conformations, especially concentrating on the splitting mode of 1274 cm^{-1}. The mode calculations are now underway in our group.

The bond rotation is facilitated by the breaking of the hydrogen bonding since the torsional strain exerted upon hydrogen bonding will be released. This hydrogen bonding seems to be formed between the carbonyl oxygen near the ethyl terminal and one of the hydrogen atoms of the PEO chain as depicted in Figure 11. To our knowledge, this is a very rare case where the hydrogen atom of PEO chain is involved in a hydrogen bonding. It is very important, here, to make an unambiguous assignment for the two free C═O groups because it provides a straightforward information about the right C═O group which participates in the hydrogen bonding. To identify the right C═O group involved in the hydrogen bonding, we replaced the ethyl terminal of 12−4 with a longer alkyl chain, which was designated as 550−22; we expected that the longer alkyl chain to prevent the hydrogen bonding due to its low mobility and steric effect. As can be seen in Figure 12 the spectrum for 550−22 shows two well-separated C═O bands. Considering the fact that when hydrogen bonding is formed the hydrogen bonded C═O mode yields a downward frequency shift,[31] the band at 1725 cm^{-1} is attributed to the hydrogen-bonded C═O mode of 1734 cm^{-1}. Thus, it is reasonable to say that the formation of the hydrogen bonding occurs preferentially with the carbonyl oxygen of ethyl ester as represented by the 1734 cm^{-1} band. The above result was further confirmed by temperature-induced change of the C═O stretching

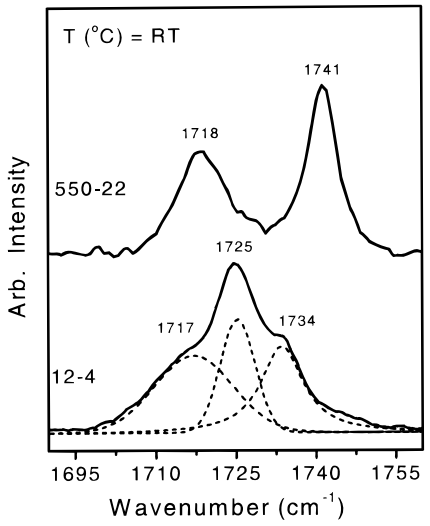

Figure 12. C═O stretching bands of 12−4 and 550−22. The obtuse profile of 12−4 is due to hydrogen bonding. The three bands with dotted line are obtained by curve-fitting of the data. The separated bands of 550−22 appear as an ethyl group is replaced by a longer alkyl chain.

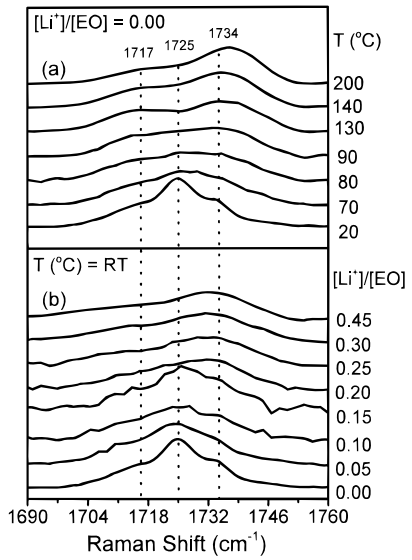

Figure 13. Profile of the C═O stretching mode with the variations of temperature (a) and salt (b).

band; the intensity of the hydrogen bonded band at 1725 cm^{-1} decreases with increasing temperature while the free C═O band at 1734 cm^{-1} increases (Figure 13a). The C═O stretching band changes in a similar manner with the variation of salt concentration (Figure 13b), implying that the intercalation of unbound salt also prevents the hydrogen bonding. One of the aromatic hydrogen atoms may be thought to form the hydrogen bonding. In such a case, the aromatic C−H stretching mode at

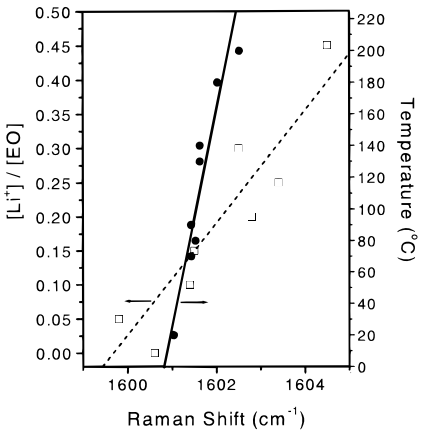

Figure 14. Frequency shifts of the C═C stretching bands as functions of temperature (●) and salt (□).

3078 cm^{-1} is anticipated to shift to higher frequency upon breaking the hydrogen bonding since a partially ionic character of the C−H bond will be restored to a single character. The result, however, shows reverse direction to the lower side (Figure 6) ruling out the hydrogen bonding by the aromatic hydrogen atoms. This downward frequency shift of this band is due to expansion of packing structure.[32] Van der Waals and dipole−dipole interactions as well as hydrogen bonding may be involved in the intermolecular interactions responsible for the stacking of the molecules. However, van der Waals and dipole−dipole interactions would be broken down simultaneously as the hydrogen bonding breaks down.

Figure 14 shows the degree of the Raman shift of the aromatic C═C bond induced by both of the temperature increase and the salt addition, in which the former results in the bigger shift to higher frequency. The temperature-dependent study is quite the contrary to the Fourier transform infrared study, in which the C═C band displays a downward shift in frequency because the magnitude and specificity of the interchain force constants generally decrease with increasing temperature.[31] The reason for the upward shift in 12−4 might be explained by taking account of the van der Waals interaction leading to $\pi-\pi$ stackings between the neighboring biphenyl rings. It seems that the $\pi-\pi$ stackings are formed between the biphenyl rings through delocalized π electrons at low temperature giving rise to the lower frequency shift. As temperature increases, van der Waals interactions will be decreased and finally broken down giving rise to the upward shift in frequency. This is due to the recovery of the electron cloud participated in the $\pi-\pi$ stackings to the C═C bond, increasing the force constant and thus the frequency. However, all the bonds in the molecule might be reduced in force constant simultaneously as the thermal energy is exerted, inducing the downward frequency shift. Concomitantly the opposite effects prevent the bigger shift. On the other hand, the addition of unbound salt plays a role only in breaking down the hydrogen bonding. Therefore, it leads to a bigger shift compared to the case of temperature increase.

4. Conclusions

To investigate the mechanism for the changes in the intermolecular interactions during the solid-to-liquid crystal transition of 12−4, salt- and temperature-dependent Raman spectra were obtained. Spectral analyses of the SO_3 stretching and the C−H stretching modes of PEO regions showed that the Li^+ ion binds to the oxygen atoms in PEO chain up to $[Li^+]/[EO] = 0.13$, while unbound salt acts as a spacer between 12−4 or 12−4 molecules and thus modifies the intermolecular packing structure in the matrix. To reveal the mechanism for the conformational change during the phase transition, we compared the spectral evolution of the combination mode of the aromatic C−C(═O)O and *C*(═O)O stretching vibrations at 1274 cm^{-1} with those of analogous molecules as a function of temperature, and found that the bond rotation occurs about the aromatic C and *C*(═O)O near the ethyl terminal. This bond rotation is considered to be facilitated mainly by the breaking of the hydrogen bonding between the carbonyl oxygen near the ethyl terminal and one of the hydrogen atoms of the PEO chain. The analysis of the C═O stretching mode allowed us to locate the right carbonyl group participated in the hydrogen bonding. The Raman shift for the aromatic C−H and aromatic C═C stretching modes further supported the loosening of the packing structure.

Acknowledgment. S.-C.Y. wishes to acknowledge the financial support from the Korea Research Foundation made in the program year 1997.

References and Notes

(1) Halperin, A. *Macromolecules* **1990**, *23*, 2724.
(2) Semenov, A. N.; Vasilenko, S. V. *Sov. Phys. JETP (Engl. Transl.)* **1986**, *63*, 70.
(3) Semenov, A. N. *Mol. Cryst. Liq. Cryst.* **1991**, *209*, 191.
(4) Williams, D. R. M.; Fedrikson, G. H. *Macromolecules* **1992**, *25*, 3561.
(5) Dias, F. B.; Voss, J. P.; Batty, S. V.; Wright, P. V.; Ungar, G. *Makromol. Chem. Rapid Commun.* **1994**, *15*, 961.
(6) Lee, M.; Oh, N.-K. *J. Mater. Chem.* **1996**, *6*, 1079.
(7) Lee, M.; Cho, B.-K.; Kim, H.; Yoon, J.-Y.; Zin, W.-C. *J. Am. Chem. Soc.* **1998**, *120*, 13258.
(8) Lee, M.; Oh, N.-K.; Lee, H. K.; Zin, W. C. *Macromolecules* **1996**, *29*, 5567.
(9) Bahadur, B. *Liquid Crystals: Applications and Uses*; World Scientific Publishing Co.: Singapore, 1990.
(10) Hummel, J. P.; Flory, P. J. *Macromolecules* **1996**, *13*, 479.
(11) Birner, P.; Kugler, S.; Simon, K.; Naray-Szabo. *Mol. Cryst. Liq. Cryst.* **1982**, *80*, 11.
(12) Lautenschlager, P.; Brickman, J.; van Ruiten, J.; Meier, R. J. *Macromolecules* **1991**, *24*, 1284.
(13) Shilov, S.; Volchek, B.; Zuev, V.; Skorokhodov, S. *Macromol. Chem. Phys.* **1994**, *195*, 865.
(14) del Pino, J.; Gomez, M. A.; Marco, C.; Ellis, G.; Fatou, J. G. *Macromolecules* **1992**, *25*, 4642.
(15) Benedetti, B.; Galleschi, F.; Chiellini, E.; Galli, G. *Polym. Phys.* **1989**, *27*, 25.
(16) Jedlinski, Z.; Franek, J.; Kulezyeki, A.; Sirigu, A.; Carfagna, C. *Macromolecules* **1989**, *22*, 1600.
(17) Kroschwitz, J. I. *Polymers: Polymer Characterization and Analysis*; John Wiley & Sons: New York, 1990.
(18) Yu, S.-C.; Paek, J.; Yu, K. H.; Ko, S. B.; Cho, I.-H.; Lee, M. *Bull. Korean Chem. Soc.* **1997**, *18*, 773.
(19) Hendra, P. Z.; Agbenyega, J. K. *The Raman Spectra of Polymers*; John Wiley & Sons: Chichester, England, 1993.
(20) Ellis, G.; Marco, C.; del Pino, J.; Lorente, J.; Gomez, M. A.; Fatou, J. G. *Vibr. Spectrosc.* **1995**, *9*, 49.
(21) del Pino, J.; Gomez, M. A.; Ellis, G.; Marco, C.; Fatou, J. G. *Macromol. Chem. Phys.* **1994**, *195*, 2049.
(22) Huang, W.; Frech, R. *Polymer* **1994**, *35*, 235.
(23) Petersen, G.; Jacobsson, P.; Torell, L. M. *Electrochim. Acta* **1992**, *37*, 1495.
(24) Yu, S.-C.; Chung, D.; Yu, K. H.; Kim, D. H.; Oh, N. K.; Lee, M.; Ko, S. B.; Cho, I. H. *Bull. Korean Chem. Soc.* **1996**, *17*, 1004.
(25) Takahashi, H.; Kyu, T.; Tran-Cong, Q.; Yano, O.; Soen, T. *J. Polym. Sci., Part B: Polym. Phys.* **1991**, *29*, 1419.
(26) Papke, B. L.; Ratner, M. A.; Shriver, D. F. *J. Phys. Chem. Solids* **1981**, *42*, 493.

(27) Maxfield, J.; Shepherd, I. W. *Polymer* **1975**, *16*, 505.
(28) Kakihana, M.; Schantz, S.; Torell, L. M.; Stevens, J. R. *Solid State Ionics* **1990**, *40/41*, 641.
(29) Czarnecki, M. A.; Katayama, N.; Satoh, M.; Watanabe, T.; Ozaki, Y. *J. Phys. Chem.* **1995**, *99*, 14101.
(30) Yu, S.-C.; Yu, K. H.; Yu, J.; Lee, M. *Bull. Korean Chem. Soc.* **1998**, *19*, 885.
(31) Wu, P. P.; Hsu, S. L.; Thomas, O.; Blumstein, A. *Polym. Phys.* **1986**, *24*, 827.
(32) Briscoe, B. J.; Stuart, B. H.; Thomas, P. S.; Williams, D. R. *Spectrochim. Acta* **1991**, *47A*, 1299.
(33) Molecular modeling was performed on a Silicon Graphics Indigo^2 Workstation to simply show the expected configuration of 12−4 when a dimer is formed. The molecular structure was obtained from Cerius^2 4.0 employing the Dreiding 2.21 force field.

MA991933M